Peptide Nucleic Acid (PNA) Amphiphiles: Synthesis, Self-Assembly, and Duplex Stability

James P. Vernille, Lara C. Kovell, and James W. Schneider*

Department of Chemical Engineering, Carnegie Mellon University, Pittsburgh, Pennsylvania 15213-3890. Received July 14, 2004

Peptide amphiphiles comprising a class of conjugates of peptide nucleic acid (PNA), natural amino acids, and *n*-alkanes were synthesized and studied. These PNA amphiphiles (PNAA) self-assemble at concentrations between 10 and 50 μM and exhibit water solubilities above 500 μM. The highly specific, stable DNA binding properties of PNAs are preserved by these modifications, with no significant differences between the thermodynamics of DNA binding of the PNA peptide and the PNA amphiphile. Proper solubilization of the PNAA required the attachment of $(Lys)_2$ and $(Glu)_4$ peptides to PNAs, which affected the PNAA–DNA duplex stability by electrostatic interactions between these charged amino acids and the negatively charged DNA backbone. These electrostatic effects did not affect the specificity of DNA binding, however. Electrostatic effects are screened with added salt, in a manner consistent with previous studies of PNA–DNA duplex stability and predictions from a charged-cylinder model for the duplex.

INTRODUCTION

Peptide nucleic acid (PNA) is a structural mimic of DNA that replaces the negatively charged sugar–phosphate backbone of DNA with an uncharged *N*-(2-aminoethyl)glycine backbone with attached nucleobases (*1*, *2*). PNA oligomers bind DNA oligomers in an antiparallel orientation, following Watson–Crick base pairing rules (*3*), but PNA–DNA duplexes are significantly more stable than the corresponding DNA–DNA duplex. The added stability of PNA–DNA duplexes has a largely electrostatic origin and is highest at low ionic strength conditions that destabilize DNA–DNA duplexes (*4*). PNA–DNA duplex stabilities are highly sensitive to sequence mismatches at the single-base level (*5*, *6*). PNA can also bind specific dsDNA targets by triplex formation, even in biological buffers that suppress triplex formation between ssDNA and dsDNA (*7*, *8*). Leveraging these unique DNA-binding properties, PNAs have been implemented in platforms for DNA sensing (*9*–*17*) and separation (*18*–*21*), primarily by linking PNAs to solid surfaces or fluorophores.

The attachment of peptides to lipophilic materials to form "peptide amphiphiles" is a convenient means to functionalize surfaces for cell attachment and proliferation (*22*, *23*) and for the measurement of molecular-level interactions between biomolecules using the atomic force microscope (AFM) (*24*) or surface force apparatus (SFA) (*25*–*27*). Surface functionalization generally requires water-insoluble peptide amphiphiles to enable Langmuir–Blodgett deposition or vesicle formation. Depending on the exact design, water-soluble peptide amphiphiles may self-assemble in solution to form disklike micelles (*28*), rodlike micelles (*29*), or helical ribbons (*30*) above their critical micelle concentration (cmc). Stupp and co-workers have shown that peptide amphiphiles can micellize with pH-dependent reversibility and that the micelles can be formed irreversibly by cross-linking of the peptide headgroups (*31*). We are working on the responsive, controlled self-assembly of peptide amphiphiles for implementation in DNA sensing and separation modalities such as liquid chromatography and capillary zone electrophoresis. With that goal in mind, we have attached *n*-alkanes and natural amino acids to form water-soluble PNA amphiphiles (PNAA). Recently, we have demonstrated that PNAA–DNA duplexes are easily separated from unbound DNA oligomers in hydrophobic interaction chromatography (*32*). The PNAA acts as a nonpolar sequence tag that helps separate target DNA from mixtures of DNA oligomers of up to 60 bases in length. Separation of longer DNA oligomers and dsDNA might be achieved with a better understanding of the binding and micellization properties of PNAA.

Because PNA is uncharged, it is sparingly soluble in water without the attachment of charged groups (*1*, *2*). For biophysical studies, either PNA oligomers are used at low concentration or a single lysine group is attached to confer greater water solubility. We expect that the attachment of *n*-alkane chains will exacerbate the poor water solubility of PNAA. For the design of PNAA, we wish to provide a moderate water solubility while maintaining sequence-specific DNA binding properties. One might expect that both the *n*-alkane and the requisite charged groups would also affect the PNAA–DNA duplex stability. For example, attachment of *n*-alkanes to collagen peptides has resulted in the stabilization of their triplexes (*33*), and the attachment of *n*-alkanes to antimicrobial peptides has been shown to promote their antimicrobial activity (*34*).

In this work, we have synthesized a series of PNAAs and measured their micellization properties and the stability of their duplexes with DNA oligomers. It should be noted that others have synthesized PNAs linked to lipophilic materials, including attachment of rhodamine and fluoroscein for thermodynamic studies (*35*) and the nonpolar group adamantane for improved cellular uptake of PNA (*36*). The distinction here is that our water-soluble PNA peptide amphiphiles have been designed for

* Author to whom correspondence should be addressed (e-mail schneider@cmu.edu).

10.1021/bc049831a CCC: $27.50
Published on Web 11/02/2004

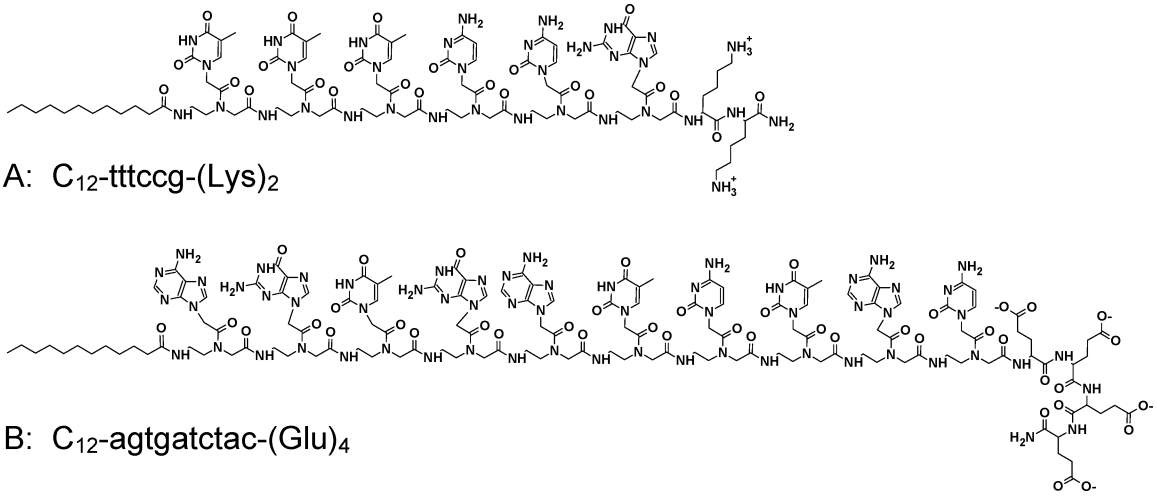

Figure 1. Structures of the PNA amphiphiles (PNAA) C_{12}-agtgatctac-$(Glu)_4$ and C_{12}-tttccg-$(Lys)_2$ used in this study. PNAA names are listed from the N to the C terminus from left to right (same binding properties as the 5′ → 3′ DNA sequence). PNAA nucleobases are in lower case.

a controlled, tunable self-assembly applicable to next-generation bioanalytical devices.

MATERIALS AND METHODS

PNAA Synthesis. All solvents (sequencing grade) were purchased from Fisher Scientific (Pittsburgh, PA), and buffers and salts were purchased from Sigma-Aldrich (St. Louis, MO). PNAAs were synthesized by solid-phase peptide synthesis using Fmoc/Bhoc-protected PNA monomers (Applied Biosystems) (*37*) and Fmoc-protected PAL-PEG-PS resin (Peptides International, Louisville, KY) with a 0.25 mmol/g loading capacity. One hundred milligrams of resin was shaken gently in dichloromethane (DCM) for several hours to expose reactive sites on the resin prior to peptide coupling. The resin was then deprotected three times with 20% piperidine in *N*,*N*-dimethylformamide (DMF) for 5 min to remove the Fmoc protecting group. A 5-fold excess of PNA monomer (based on manufacturer's reported loading capacity) in base solution (Applied Biosystems) and activator solution (Applied Biosystems) was then prepared (*38*), The base solution consists of a mixture of 2,6-lutidine and *N*,*N*-diisopropylethylamine in DMF. The activator is a solution of *O*-(7-azabenzotriazol-1-yl)-1,1,3,3-tetramethyluronium hexafluorophosphate (HATU) in DMF. Following a 2-min activation step, the solution was added to the resin. The initial monomer coupling to resin was allowed to proceed for at least 1 h to ensure complete coupling on the optimal number of resin sites. We found that the longer coupling time was required for high yields. The resin was washed with DCM and DMF following the coupling step and a small fraction collected for a ninhydrin test. Unreacted sites were then capped by a 10-min incubation of the resin with the acetic anhydride. The resin was washed with DCM and DMF, and the process was repeated with 20-min coupling steps until the desired PNA peptide was synthesized. Lauric acid (Sigma-Aldrich) was then coupled to the N terminus of the PNA peptide, also in a 5-fold excess.

The resin was soaked in a mixture of 4:1 trifluoroacetic acid (TFA)/*m*-cresol (total volume = 2 mL) for 2 h to cleave the PNAA from the resin and remove Bhoc side protecting groups. Once cleaved from the support, the PNAA was precipitated by the addition of dry ether (~10-fold excess over PNAA). The precipitated PNAA was cooled for 5 min in a −80 °C freezer to ensure complete precipitation. The solid was separated from the ether by centrifugation (1000*g*) for 5 min. The top phase was decanted off and the pellet resuspended with another addition of dry ether. The cooling and centrifugation process was done in triplicate. Upon completion, the PNAA pellet was dried within a stream of nitrogen and dissolved in deionized water. In many cases, yields of PNAA were improved substantially by foregoing the ether precipitation step and injecting the cleavage cocktail directly into the HPLC for purification.

Semipreparative-scale PNAA purification was performed on a Waters Delta 600 HPLC using a Symmetry300 C_4 column with a particle size of 5 μm. Elution of the PNAA product was achieved using a 30-min linear gradient (0.1% TFA in acetonitrile to 0.1% TFA in water) and a 20 mL/min flow rate. The product eluted as a single peak and following collection was lyophilized to a powder. The yield of the reaction was ~30% (based on the manufacturer's reported resin loading), or 0.0075 mmol of PNAA product. The following $[M + H]^+$ values for PNA peptides and PNAA amphiphiles were obtained: C_{12}-tttccg-$(Lys)_2$, 2050 Da (theoretical: 2049.96); NH_2-tttccg-$(Lys)_2$, 1865.91 Da (theoretical: 1866.71); C_{12}-agtgatctac-$(Glu)_4$, 3425.8 Da (theoretical: 3425.52); NH_2-agtgatctac-$(Glu)_4$, 3242.52 Da (theoretical: 3241.59).

The naming convention we use lists the PNA peptide sequence in the N to C direction from left to right (Figure 1). PNA sequences listed in the N to C direction follow the same Watson−Crick base pairing rules as the corresponding DNA sequence listed in the 5′ to 3′ direction. Note that the resin used here leaves a terminal amine group at the C terminus. PNA nucleobases are in lower case to distinguish them from DNA nucleobases (upper case). The three-letter abbreviation is used for the natural amino acids, and the length of *n*-alkane is the subscript under "C."

Solubility Measurements. PNAA solubilities were measured by centrifugation of saturated PNAA solutions in buffer. A large (>1 mM) amount of PNAA was dissolved in 20 mM sodium phosphate buffer (pH 7.0) and cooled to 4 °C. Samples were then warmed to room temperature and centrifuged (Eppendorf 5415C microcentrifuge) to sediment aggregated or precipitated material. The PNAA concentration in the supernatant was measured spectrophotometrically on a Varian Cary 3 spectrophotometer at 260 nm. PNAA concentrations were calculated from the measured absorbance by Beer's law. Extinction coefficients for the PNAA were calculated by

summing the extinction coefficients for each monomer on the PNA peptide (ϵ_{260} = 13700, 11700, 8600, and 6600 L/mol-cm for A, G, T, and C, respectively.) Absorbance measurements were made at 80 °C to ensure that the nucleobases were completely destacked and that hypochromicity could be neglected.

cmc Measurements. Critical micelle concentrations for the PNAA were obtained by light scattering using a Malvern Zetasizer 3000 system (Malvern Instruments). Solutions of PNAA in 20 mM sodium phosphate buffer (pH 7.0) were prepared and filtered to remove dust or large PNAA aggregates using 0.2-μm syringe filters (Fisher). UV absorbance measurements were made on the filtrate to account for any losses of PNAA during filtration. The filtered solutions were then placed in a 1-mL cuvette and installed in the Zetasizer instrument. The intensity of laser light (532 nm) scattered 90° from incidence was measured using an internal photomultiplier and recorded by the Zetasizer software. Disposable cuvettes were used to obviate any carry-over of PNAA from sample to sample. The cmc was taken to be the PNAA concentration at which the intensity versus [PNAA] plot had a pronounced slope discontinuity.

UV Melting Curves and Circular Dichroism (CD). DNA oligomers were purchased from Integrated DNA Technologies (Coralville, IA) and used as received. DNA purity was assessed using anion-exchange chromatography (Waters Spherisorb S5 SAX column, 80-Å pore size and 5-μm particle size), with a 30-min linear gradient from 20 mM Tris-HCl (pH 8.0) to 20 mM Tris-HCl in 1 M NaCl (pH 8.0). Samples with purity of <95% were rejected. Stock solutions of DNA oligomers were prepared in 20 mM phosphate buffer (pH 7.0) for UV melting analysis.

CD spectra were run on a Jasco J-715 spectropolarimeter equipped with a thermoelectrically controlled single-cell holder. CD spectra for PNAA−DNA mixtures were obtained in 5 mM sodium phosphate buffer (pH 7.0) with 100 mM NaCl and 1 mM EDTA.

UV melting curves were obtained at 260 nm for PNAA−DNA solutions in 20 mM sodium phosphate buffer (pH 7.0) using a Varian Cary 3 spectrophotometer equipped with a thermoelectrically controlled multicell holder using 1-cm quartz cuvettes (Starna, Atascadero, CA). PNAA−DNA mixtures were initially heated to 90 °C and held there for 2 min to equilibrate. The temperature was then lowered at 1.0 °C/min to a lower target value (5−20 °C) and cycled between the upper and lower temperature limits several times.

Melting temperatures and thermodynamic data for all melting curves were determined by a van't Hoff analysis under a two-state model for hybridization

$$S_{PNA} + S_{DNA} \leftrightarrow D_{PNA/DNA} \quad (1)$$

where S denotes single strands and D duplex. The two-state model is considered to be valid for short sequences (4−20 base pairs) (*39*). The absorbance versus temperature plot is converted to a plot of duplex fraction (α) versus temperature. The total absorbance (A) is assumed to be the sum of the absorbance of the single strands (A_S) and the double strands (A_D):

$$A = \alpha A_D + (1 - \alpha)A_S \quad (2)$$

The melting transition temperature (T_m) is taken to be the temperature at which $\alpha = 0.5$. The absorbance values of the single- and double-stranded forms of the DNA and PNA are assumed to vary linearly with temperature and take the form

$$A_S = m_S T + b_S$$
$$A_D = m_D T + b_D \quad (3)$$

As nucleotide length increases, the nucleobase stacking dynamics become more pronounced and the slopes m_S and m_D will deviate from zero.

The equilibrium constant for the hybridization process is

$$K = \frac{[D_{PNA/DNA}]}{[S_A][S_B]} = \frac{2\alpha}{(1 - \alpha)^2 C_T} \quad (4)$$

where C_T is the total concentration of strands, on a single-strand basis. The equilibrium constant, K, versus temperature data can be analyzed using the van't Hoff equation to obtain the enthalpy of hybridization ΔH

$$\frac{d \ln K}{d(1/T)} = \frac{-\Delta H^\circ}{R} \quad (5)$$

where R is the gas constant.

RESULTS AND DISCUSSION

PNAA Synthesis. Most PNA syntheses have been accomplished by solid-phase synthesis using Boc/Z-protected monomers following the protocol of Christensen et al. (*40*). In our case, we were interested in attaching dialkyl chains with ester linkages that are hydrolyzed under the cleavage conditions required for Boc/Z. The milder cleavage conditions required by Fmoc/Bhoc protection have been shown to maintain the ester linkage (*41*), and therefore we used the Fmoc/Bhoc approach. The Fmoc/Bhoc PNA synthesis protocol provided by Egholm and Casale (*42*) was developed for automated PNA synthesis, and it was refined for manual synthesis in our laboratory. The most significant changes were increasing the coupling, capping, and deprotection times and the use of a 5-fold excess of monomer for each coupling. To obtain high yields, we found it necessary to increase the time of the initial resin−monomer coupling to 1 h, but subsequent couplings could be performed for 20 min. Because the alkane-modified PNAs are more nonpolar than the PNA peptides, it was often necessary to inject the cleavage cocktail directly into the HPLC for high-yield purification. The PNAA structures we are mainly concerned with in this paper are listed in Figure 1.

Solubility and cmc Measurements. Unmodified PNAs are sparingly soluble in water and have a tendency to self-aggregate even when the PNAs are apparently solubilized (*2*). A typical approach to improve water solubility is attachment of a C-terminal lysine residue to the sequence, which for the PNA peptide NH_2-t_{10}-Lys confers a water solubility of >1.5 mM in 10 mM sodium phosphate buffer (pH 7.0) (*37*). For PNAA, additional charges need to be added to bring the solubility of PNAA above their cmc, enabling self-assembly. To find an appropriate combination of alkane substitution and charging, we synthesized about 12 variants with different PNA sequences and substitutions. The PNAAs C_{18}-tttccg-Lys, C_{16}-tttccg-Lys, and C_{14}-tttccg-Lys gave a cloudy solution at 1−10 μM concentrations in water or 10 mM sodium phosphate buffer (pH 7.0). C_{12}-tttccg-$(Lys)_2$ had twice the solubility of C_{12}-Lys-tttccg-Lys and was studied in more detail (Figure 1A). For longer PNA sequences, such as C_{12}-t_{10}-$(Lys)_4$ in 20 mM phosphate buffer (pH 7.0),

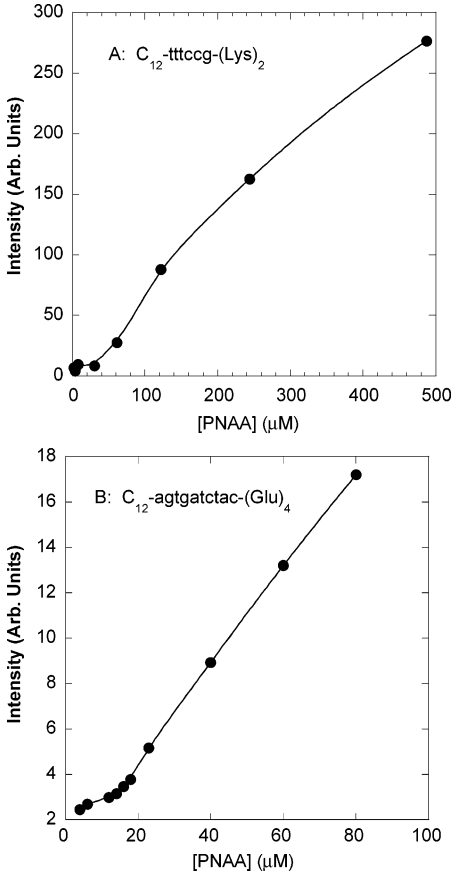

Figure 2. Scattered intensity versus [PNAA] for (A) C_{12}-tttccg-$(Lys)_2$ and (B) C_{12}-agtgatctac-$(Glu)_4$ in 20 mM sodium phosphate buffer (pH 7.0). The cmc is marked by an abrupt increase in scattered intensity (*43*).

Table 1. Solubilities and Critical Micelle Concentrations for PNA Amphiphiles in 20 mM Phosphate Buffer (pH 7.0)

	solubility, 25 °C (μM)	cmc, 25 °C (μM)
C_{12}-tttccg-$(Lys)_2$	1000	40
C_{12}-agtgatctac-$(Glu)_4$	650	15

addition of either complementary or noncomplementary DNA to 20 mM phosphate buffer clouded the solution. The clouding was mitigated by the use of glutamic acid groups to charge the PNAA, the use of a Tris-HCl (pH 7−8) buffer rather than phosphate buffer, or adjusting the pH to pH ∼2−3. The PNAA C_{12}-agtgatctac-$(Glu)_4$ (Figure 1B) has a solubility of 1000 μM in 20 mM sodium phosphate buffer and >1400 μM in 10 mM Tris-HCl (pH 7.0).

Although the effect of tail length, charge amount and type, and length of PNA sequence have not been exhaustively studied, some rules of thumb have emerged. Generally, 6-mer sequences require two charged groups and 10-mer sequences require four charged groups for solubilities on the order of 500−1000 μM. Charged groups placed at the N terminus of the PNA peptide were more effective than those placed between the alkane and the PNA peptide.

cmc measurements were made by a light-scattering method using a laser Doppler velocimetry system in static mode. The cmc is marked by a large increase in scattered intensity as shown in Figure 2 (*43*). The shorter PNAA sequence of C_{12}-tttccg-$(Lys)_2$ gave a slightly higher cmc than C_{12}-agtgatctac-$(Glu)_4$ (Table 1). cmc values for C_{14}-tttccg-$(Lys)_2$ and C_{18}-tttccg-$(Lys)_2$ were similar to that of C_{12}-tttccg-$(Lys)_2$, indicating that the primary driving force

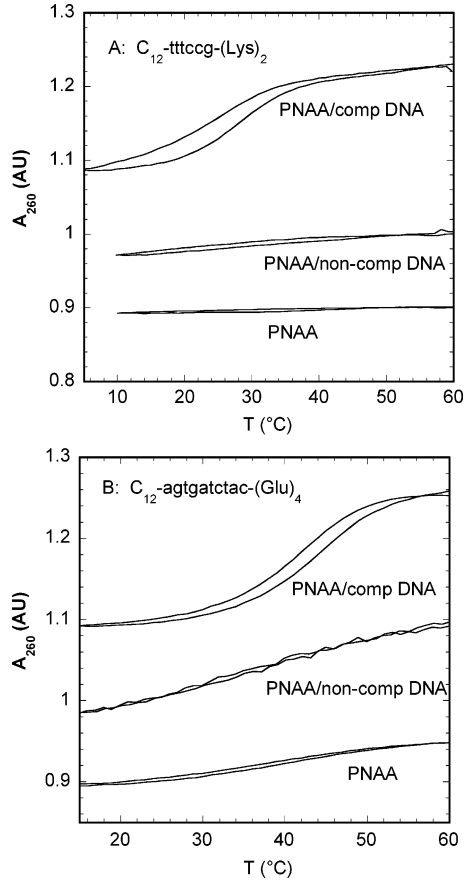

Figure 3. UV melting curves for PNAA with and without DNA: (A) C_{12}-tttccg-$(Lys)_2$ alone, with noncomplementary DNA (5′-ATAGCC-3′), and with complementary DNA (5′-CGGAAA-3′); (B) C_{12}-agtgatctac-$(Glu)_4$ alone, with noncomplementary DNA (5′-TGTACGACTC-3′), and with complementary DNA (5′-GTAGATCACT-3′). For (A) and (B), a ramp rate of 1.0 °C/min and a total strand concentration of 20 μM in 20 mM sodium phosphate at pH 7.0 were used. In each case, the self-melt was shifted up by 0.4 AU and the PNAA/noncompDNA was shifted down by 0.1 AU for clarity.

for micellization is attractive interactions between the PNA peptides. Accordingly, longer sequences tend to lower the cmc. To avoid complications, the measurements presented below were made at concentrations below the cmc for both PNAA.

Hybridization of PNA Amphiphiles with DNA. The substitutions made on the PNA peptide to form PNAA include the *n*-alkane tail and the charged amino acids, and both could potentially affect the specificity of binding to DNA oligomers and the stability of the resulting PNAA−DNA duplex. Figure 3A shows UV melting curves for the PNAA C_{12}-tttccg-$(Lys)_2$ with an equimolar amount of its 6-mer DNA complement (5′-CGGAAA-3′), a noncomplementary 6-mer (5′-ATAGCC-3′), and the PNAA on its own. Significant hypochromicity was observed only for the PNAA/complementary DNA mixture (T_m = 27.6 °C), indicating sequence specificity is preserved. Figure 3B shows UV melting curves for the PNAA C_{12}-agtgatctac-$(Glu)_4$ with an equimolar amount of its 10-mer DNA complement (5′-GTAGATCACT-3′), a noncomplementary 10-mer (5′-TGTACGACTC-3′), and the PNAA on its own. In this case, each of the three curves shows hypochromicity. A van't Hoff analysis of the PNAA/complementary DNA curve gave T_m = 42.0 °C. Other hypochromicities are likely due to self-melt characteristics for the longer DNA and PNAAs of Figure 3B. Self-melts are generally larger for PNAs compared to

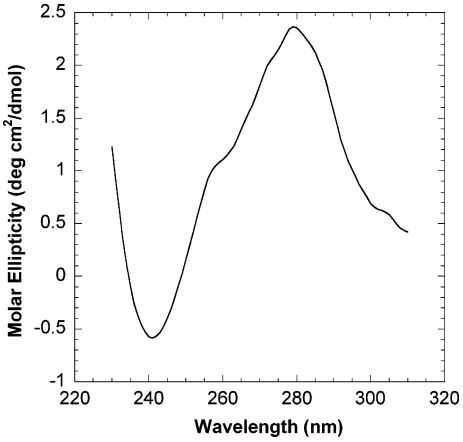

Figure 4. CD spectrum for C_{12}-agtgatctac-$(Glu)_4$ with 5′-GTAGATCACT-3′ at a total strand concentration of 5 μM (averaged over 10 scans) 20 mM sodium phosphate at pH 7.0 (T = 25 °C).

Table 2. Melting Temperatures for PNAA with Complementary DNA Targets (5′-CGGAAA-3′ and 5′-GTAGATCACT-3′) in 20 mM Phosphate Buffer (pH 7.0), along with T_m Predictions from a Nearest-Neighbor Model (*45*)

	T_m (°C),[a] exptl	T_m (°C), theor
NH_2-tttccg-$(Lys)_2$	27.4	24.3
C_{12}-tttccg-$(Lys)_2$	27.6	24.3
NH_2-agtgatctac-$(Glu)_4$	38.9	53.7
C_{12}-agtgatctac-$(Glu)_4$	42.0	53.7

[a] T_m had an associated error of 0.5 °C.

DNAs as the more flexible PNA backbone allows the nucleobases to stack to a greater degree. Because the hypochromicity is comparable for the PNAA and the PNAA with noncomplementary DNA, we conclude that the mixture does not form a duplex or other intermolecular association. This self-structured nature of the C_{12}-agtgatctac-$(Glu)_4$ can be considered a small potential source of error when the melting curve for thermodynamic parameters is analyzed. Note that the self-melt is not evident in the case of the shorter PNAA and DNA 6-mers (Figure 3A). A small hysteresis between the melting and cooling curves was observed in each case. For the C_{12}-agtgatctac-$(Glu)_4$ PNAA−DNA melting curve, the hysteresis decreased from 1.54 to 0.41 °C when the scan rate was slowed from 1 to 0.5 °C/min.

To verify duplex formation, the secondary structure of the PNAA−DNA duplex was confirmed using CD (Figure 4). Hybridization of C_{12}-agtgatctac-$(Glu)_4$ with complementary DNA 5′-GTAGATCACT-3′ shows the formation of a right-handed helix with maxima at 260 and 280 nm and a minimum at 240 nm. These features compare well with those measured by Ratilainen (*35*) for a PNA peptide with a single lysine group attached. CD spectra were not obtained for the duplex of C_{12}-tttccg-$(Lys)_2$ and its 6-mer DNA complement, since the duplex is marginally stable in phosphate buffer at room temperature.

UV melting curves were also obtained for the corresponding PNA peptides without alkylation and are summarized in Table 2. For both PNAAs studied here, the corresponding peptide shows about the same T_m. Similar observations have been made by Griffin and Smith (*44*) for PNAs with attached 8-amino-3,6-dioxaoctadecanoic acid groups and by Ørum et al. (*18*) for PNAs with attached $(His)_6$ peptides. Although alkylation appears to have little effect on the binding, the substantial amount of charged amino acids required for solubilization does.

Table 3. Thermodynamic Parameters for Hybridization of PNAA C_{12}-agtgatctac-$(Glu)_4$ with Complementary DNA (5′-GTAGATCACT-3′) in 10 mM Tris Buffer (pH 7.0, unless Otherwise Indicated) with Increasing Concentrations of NaCl[a]

[NaCl] (mM)	T_m (°C)	ΔH (kJ/mol)	ΔG_{298} (kJ/mol)
0 (pH 4.0)	41.7	−256	−45.7
0	39.7	−274	−45.0
20	42.7	−254	−46.2
40	43.8	−265	−47.8
60	44.5	−277	−49.2
80	45.0	−270	−49.1
100	45.3	−286	−50.3
1000	47.2	−300	−52.9

[a] T_m had an associated error of 0.5 °C, ΔH had an error of 10 kJ/mol, and ΔG had an error of 0.5 kJ/mol.

Giesen et al. (*45*) provided an extension to the nearest-neighbor model of SantaLucia (*46*) for PNA−DNA duplexes. The model claims to be valid over a wide range of ionic strengths and does not include the effects of amino acids or lipids and, hence, serves as a useful reference. Table 2 includes a comparison of the model predictions and the observed T_m and shows that T_m is underpredicted in the case of C_{12}-tttccg-$(Lys)_2$ and overpredicted in the case of C_{12}-agtgatctac-$(Glu)_4$, pointing to an electrostatic contribution to the duplex stability.

To verify the electrostatic nature of the stabilization in the case of C_{12}-tttccg-$(Lys)_2$ and destabilization in the case of C_{12}-agtgatctac-$(Glu)_4$, the effect of added salt on PNAA−DNA duplex stability was determined for C_{12}-agtgatctac-$(Glu)_4$ (Table 3). As the ionic strength was increased (pH 7.0), T_m increased and ΔG decreased as expected. Additionally, the duplex was stabilized by decreasing the pH to 4.0 (no added salt), likely due to the lowering state of charging for the Glu residues, the side-chain carboxylic acid of which has a pK_a of 4.07. Below pH 4.0, UV spectra were excessively noisy due to light scattering from insoluble aggregates of PNAA.

The effect of ionic screening on PNAA−DNA duplex stability can be predicted by a Poisson−Boltzmann-type model (*47*, *48*) that considers the oligomers to behave as charged cylinders with a higher charge density in duplex form than as a single-stranded coil. An increase in bulk cation concentration acts to stabilize the high charge density state, resulting in a higher thermal stability. The change in melting temperature with changing salt concentration can be related to the thermodynamic differential counterion association parameter per phosphate group ($\Delta\psi$) by (*4*, *49*)

$$\frac{dT_m}{d\log[Na^+]} = 0.9\left\{\frac{2.03RT_m^2}{\Delta H}\right\}(N_u\Delta\psi) \qquad (6)$$

where ΔH is the helix-to-coil transition enthalpy, R is the gas constant with units of cal/(mol K), and N_u is the number of charged groups (phosphate, in the case of DNA) per cooperative melting unit. The data of Table 3 have $dT_m/d\log[Na^+]$ for C_{12}-agtgatctac-$(Glu)_4$ of 3.8 K, indicating that counterion association takes place upon PNA−DNA helix formation. From ΔH and T_m values taken from the van't Hoff analysis of the melting curves, the thermodynamic differential counterion association parameter ($\Delta\psi$) was calculated to be 0.059.

Table 4 summarizes these results and compares them to literature values. Because the PNAA C_{12}-tttccg-$(Lys)_2$ has a low T_m, it was difficult to obtain the full sigmoidal curve required for accurate thermodynamic data in the presence of added salt. Instead, we measured melting

Table 4. Salt Concentration Dependence on Duplex Stability for PNAA with Complementary DNA (5′-CGGAAA-3′ and 5′-GTAGATCACT-3′) in 10 mM Tris Buffer (pH 7.0)

duplex	$d(T_m)/d(\log[Na^+])$ (K)	$RT_m^2/\Delta H$ (K)	$\Delta\psi$ (mol/mol of duplex)
C_{12}-tttccg-$(Lys)_2$−DNA	−4.2	1.95	−0.17
C_{12}-agtgatctac-$(Glu)_4$−DNA	3.8	3.10	0.059
PNA−DNA[a]	−3.4	3.52	−0.05
DNA−DNA[a]	15.9	2.74	0.15

[a] Literature values for PNA and DNA decamers and their DNA−decamer complements (*4*).

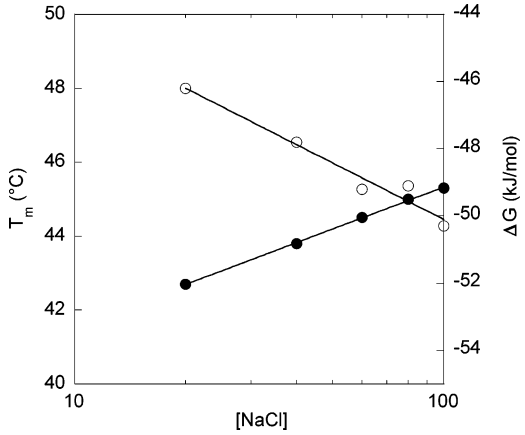

Figure 5. Dependence of T_m (filled circles) and ΔG (open circles) on the concentration of NaCl added to 10 mM Tris buffer for hybridization of PNAA C_{12}-agtgatctac-$(Glu)_4$ with complementary DNA (5′-GTAGATCACT-3′). The T_m data are fit to the equation $T_m = 37.8 + 3.77\log([Na^+])$, and the ΔG data are fit to the equation $\Delta G = -38.9 - 5.58\log([Na^+])$. Regression coefficients are >98% in both cases.

curves in pure water (deemed to have an effective $[Na^+] = 10^{-5}$ M) and compared them to the buffer case (effective $[Na^+] = 2 \times 10^{-2}$ M). In this case, $\Delta\psi = -0.17$, indicating that counterions are released on duplex formation owing to the complexation of positively charged lysine and negatively charged phosphates. Tomac et al. (*4*) made similar measurements and obtained a value of $\Delta\psi = -0.05$ for an unmodified PNA 10-mer with fully complementary DNA and $\Delta\psi = 0.15$ for the corresponding DNA−DNA duplex. This indicates that the addition of 4 Glu residues has the same destabilizing effect as about 2.5 phosphate groups. Although each group carries a negative charge, in principle, this result is reasonable considering the separation between the distal Glu groups and DNA phosphate groups and the possibility of incomplete dissociation of the side-group carboxylic acids at pH 7.0. Figure 5 is a plot of T_m and ΔG with added salt, showing a semilog dependence. Griffin and Smith obtained a value of $d\Delta G/d\log[Na^+] = -1.82$ kJ/mol for fully complementary PNA (unmodified) and DNA 9-mers. The PNA−DNA duplex is stabilized by added salt, because

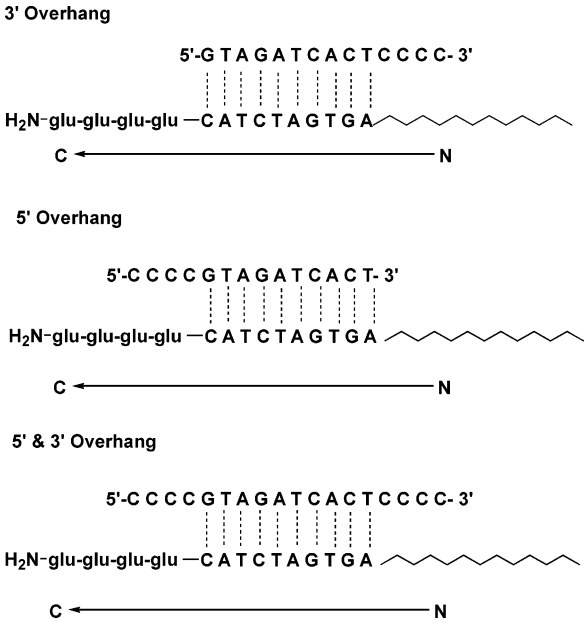

Figure 6. Orientation of the PNAA/DNA duplex with overhanging DNA bases on the 3′, 5′, and 3′ and 5′ ends.

the helix carries a greater charge density than the coil, as described above. We obtained a value of $d\Delta G/d\log[Na^+] = -5.58$ kJ/mol, indicating a much greater free energy penalty for the introduction of $(Glu)_4$ to the duplex than the closer proximity of phosphate charges required for helix formation.

Datta and Armitage have reported a stabilizing effect of overhanging, unbound DNA bases on PNA−DNA duplexes with length asymmetries (*50*). The overhang effect was ascribed to an enthalpic gain provided by stacking of the overhanging DNA bases with those in the PNA−DNA duplex. The effect is more evident in PNA−DNA duplexes than in DNA−DNA duplexes, presumably due to the wider pitch of the PNA−DNA helix that leaves bases more exposed to solvent. To determine if the alkane tail would have any impact on overhang-induced stabilization, we also collected UV-melting data using longer DNA strands, those with overhanging C bases surrounding a 10-mer binding site (Table 5; Figure 6). The first conclusion we draw is that, for overhangs on both sides of the PNAA binding sequence of the DNA, there appears to be no difference for the PNA peptide compared to the PNA amphiphile. Additionally, DNA overhangs on the 3′ end of the binding sequence (closest to the PNAA alkane, Figure 6) stabilize the duplex while those on the 5′ end (closest to the $(Glu)_4$ group, Figure 6) destabilize the PNAA−DNA duplex. Because the thermodynamic data for PNAA−DNA duplexes mirror those for PNA−DNA duplexes, we must presume that the stabilization afforded by the 3′ overhangs is due to the same effect reported by Datta and Armitage, whereas the destabilization by the 5′ overhangs has an electrostatic origin that

Table 5. Effect of Overhang Position on Thermodynamic Parameters for Duplexes of Various DNA Oligomers and the PNA Amphiphile C_{12}-agtgatctac-$(Glu)_4$ or the PNA Peptide NH_2-agtgatctac-$(Glu)_4$[a]

DNA target (3′→5′)	T_m (°C), amph	T_m (°C), peptide	ΔH (kJ/mol), amph	ΔH (kJ/mol), peptide	ΔG_{298} (kJ/mol), amph	ΔG_{298} (kJ/mol), peptide
TCACTAGATG	42.0	38.9	−287	−264	−47.7	−43.7
TCACTAGATG**CCCC**	37.3	38.7	−181	−163	−37.3	−38.7
CCCCTCACTAGATG	47.8	47.7	−298	−292	−53.1	−52.7
CCCCTCACTAGATG**CCCC**	45.0	45.4	−281	−287	−49.8	−50.6
CCCCCCTCACTAGATG**CCCCCC**	50.1		−328		−57.6	
CCCCCCCCTCACTAGATG**CCCCCCCC**	50.4		−329		−58.0	

[a] Overhanging DNA bases are in bold (see Figure 6).

either exists along with an overhang stabilization (but outweighing it) or prevents the molecular arrangements required for overhang stabilization from occurring. Finally, we note that the overhang-induced stabilization appears to saturate with six cytosine bases on each end of the binding sequence, because the stability is not improved with eight bases on each end. This appears to agree with results from Datta and Armitage, who found a significant added stabilization of PNA−DNA duplexes with eight overhanging bases rather than four.

CONCLUSIONS

We have provided details concerning the synthesis and characterization of PNA amphiphiles (PNAA), self-assembling compounds that bind DNA with high selectivity. We have found that the addition of the alkane tail makes self-assembly possible, but does not affect the binding selectivity or the stability of the resulting PNAA−DNA duplex. The incorporation of about four charged amino acids per 10-mer (or two per 6-mer) was required for adequate water solubility. Addition of a $(Glu)_4$ peptide destabilized the duplex, whereas addition of a $(Lys)_2$ peptide stabilized it. Both effects were attenuated with increased ionic strength, indicating an electrostatic mechanism. This electrostatic control over the stability could be useful for the tuning of the duplex melting temperature for future applications of these materials in bioanalytical devices. Stabilization of the PNAA−DNA duplex was also observed when using DNAs with overhanging bases, but this overhang stabilization was not affected by the PNAA alkane.

ACKNOWLEDGMENT

We acknowledge the National Science Foundation (BES-0093538), the Arnold and Mabel Beckman Foundation, and a joint grant from the Air Force Office of Scientific Research and the DARPA SIMBIOSYS program for financial support of this work. We also thank Bruce Armitage and Stu Kushon for helpful discussions.

LITERATURE CITED

(1) Nielsen, P. E. (1999) Peptide nucleic acid. A molecule with two identities. *Acc. Chem. Res. 32*, 624−630.

(2) Uhlmann, E.; Peyman, A.; Breipohl, G.; Will, D. W. (1998) PNA: synthetic polyamide nucleic acids with unusual binding properties. *Angew. Chem., Int. Ed. Engl. 37*, 2796−2823.

(3) Egholm, M.; Buchardt, O.; Christensen, L.; Behrens, C.; Freier, S. M.; Driver, D. A.; Berg, R. H.; Kim, S. K.; Norden, B.; Nielsen, P. E. (1993) PNA hybridizes to complementary oligonucleotides obeying the Watson−Crick hydrogen-bonding rules. *Nature 365*, 566−568.

(4) Tomac, S.; Sarkar, M.; Ratilainen, T.; Wittung, P.; Nielsen, P. E.; Norden, B.; Graslund, A. (1996) Ionic effects on the stability and conformation of peptide nucleic acid complexes. *J. Am. Chem. Soc. 118*, 5544−5552.

(5) Igloi, G. L. (1998) Variability in the stability of DNA-peptide nucleic acid (PNA) single-base mismatched duplexes: real-time hybridization during affinity electrophoresis in PNA-containing gels. *Proc. Natl. Acad. Sci. 95*, 8562−8567.

(6) Ratilainen, T.; Holmén, A.; Tuite, E.; Nielsen, P. E.; Nordén, B. (2000) Thermodynamics of sequence-specific binding of PNA to DNA. *Biochemistry 39*, 7781−7791.

(7) Kim, S. K.; Nielsen, P. E.; Egholm, M.; Buchardt, O.; Berg, R. H.; Norden, B. (1993) Right-handed triplex formed between peptide nucleic acid PNA-T8 and poly(dA) shown by linear and circular dichroism spectroscopy. *J. Am. Chem. Soc. 115*, 6477−6481.

(8) Wittung, P.; Nielsen, P.; Nordén, B. (1996) Direct observation of strand invasion by peptide nucleic acid (PNA) into double-stranded DNA. *J. Am. Chem. Soc. 118*, 7049−7054.

(9) Ørum, H.; Nielsen, P. E.; Egholm, M.; Berg, R. H.; Buchardt, O.; Stanley, C. (1993) Single base pair mutation analysis by PNA directed PCR clamping. *Nucleic Acids Res. 21*, 5332−5336.

(10) Gaylord, B. S.; Heeger, A. J.; Bazan, G. C. (2002) DNA hybridization detection with water-soluble conjugated polymers and chromophore-labeled single-stranded DNA. *J. Am. Chem. Soc. 125*, 896−900.

(11) Komiyama, M.; Ye, S.; Liang, X.; Yamamoto, Y.; Tomita, T.; Zhou, J.-M.; Aburatani, H. (2003) PNA for one-base differentiating protection of DNA from nuclease and its use for SNPs detection. *J. Am. Chem. Soc. 125*, 3758−3762.

(12) Wang, J.; Palecek, E.; Nielsen, P. E.; Rivas, G.; Cai, X.; Shiraishi, H.; Dontha, N.; Luo, D.; Farias, P. A. M. (1996) Peptide nucleic acid probes for sequence-specific DNA biosensors. *J. Am. Chem. Soc. 118*, 7667−7670.

(13) Wang, J.; Nielsen, P. E.; Jiang, M.; Cai, X.; Fernandes, J. R.; Grant, D. H.; Ozsoz, M.; Beglieter, A.; Mowat, M. (1997) Mismatch-sensitive hybridization detection by peptide nucleic acids immobilized on a quartz crystal microbalance. *Anal. Chem. 69*, 5200−5302.

(14) Wang, J.; Rivas, G.; Cai, X.; Chicharro, M.; Parrado, C.; Dontha, N.; Begleiter, A.; Mowat, M.; Palecek, E.; Nielsen, P. E. (1997) Detection of point mutation in the p53 gene using a peptide nucleic acid biosensor. *Anal. Chim. Acta 344*, 111−118.

(15) Myal, Y.; Blanchard, A.; Watson, P.; Corrin, M.; Shiu, R.; Iwasiow, B. (2000) Detection of genetic point mutations by peptide nucleic acid-mediated Polymerase Chain Reaction clamping using paraffin-embedded specimens. *Anal. Biochem. 285*, 169−172.

(16) Ross, P. L.; Lee, K.; Belgrader, P. (1997) Discrimination of single-nucleotide polymorphisms in human DNA using peptide nucleic acid probes detected by MALDI-TOF mass spectrometry. *Anal. Chem. 69*, 4197−4202.

(17) Svanvik, N.; Westman, G.; Wang, D.; Kubista, M. (1999) Light-Up probes: thiazole orange-conjugated peptide nucleic acid for detection of target nucleic acid in homogeneous solution. *Anal. Biochem. 281*, 26−35.

(18) Ørum, H.; Nielsen, P. E.; Jorgensen, M.; Larsson, C.; Stanley, C.; Koch, T. (1995) Sequence-specific purification of nucleic acids by PNA-controlled hybrid selection. *BioTechniques 19*, 472−480.

(19) Seeger, C.; Batz, H.-G.; Ørum, H. (1997) PNA-mediated purification of PCR amplifiable human genomic DNA from whole blood. *BioTechniques 23*, 512−517.

(20) Chandler, D. P.; Stults, J. R.; Cebula, S.; Schuck, B. L.; Weaver, D. W.; Anderson, K. K.; Egholm, M.; Brockman, F. J. (2000) Affinity purification of DNA and RNA from environmental samples with peptide nucleic acid clamps. *Appl. Environ. Microbiol. 66*, 3438−3445.

(21) Chandler, D. P.; Stults, J. R.; Anderson, K. K.; Cebula, S.; Schuck, B. L.; Brockman, F. J. (2000) Affinity capture and recovery of DNA at femtomolar concentrations with peptide nucleic acid probes. *Anal. Biochem. 283*, 241−249.

(22) Winger, T. M.; Ludovice, P. J.; Chaikof, E. L. (1996) Lipopeptide conjugates: biomolecular building blocks for receptor activating membrane-mimetic structures. *Biomaterials 17*, 437−441.

(23) Dori, Y.; Bianco-Peled, H.; Satija, S. K.; Fields, G. B.; McCarthy, J. B.; Tirrell, M. (2000) Ligand accessibility as means to control cell response to bioactive bilayer membranes. *J. Biomed. Mater. Res. 50*, 75−81.

(24) Dillow, A. K.; Ochsenhirt, S. E.; McCarthy, J. B.; Fields, G. B.; Tirrell, M. (2001) Adhesion of $\alpha 5\beta 1$ receptors to biomimetic substrates constructed from peptide amphiphiles. *Biomaterials 22*, 1493−1505.

(25) Schneider, J.; Berndt, P.; Haverstick, K.; Kumar, S.; Chiruvolu, S.; Tirrell, M. (1998) Force and adhesion measurements between hydrogen-bonded layers of glycine-functionalized amphiphiles. *J. Am. Chem. Soc. 120*, 3508−3509.

(26) Berndt, P.; Kurihara, K.; Kunitake, T. (1995) Measurement of forces between surfaces composed of two-dimensionally organized, complementary and noncomplementary nucleobases. *Langmuir 11*, 3083−3091.

(27) Pincet, F.; Perez, E.; Bryant, G. (1996) Specific forces between DNA bases. *Mod. Phys. Lett. B 10*, 81−99.
(28) Gore, T.; Dori, Y.; Talmon, Y.; Tirrell, M.; Bianco-Peled, H. (2001) Self-assemply of model collagen peptide amphiphiles. *Langmuir 17*, 5352−5360.
(29) Hartgerink, J. D.; Beniash, E.; Stupp, S. I. (2001) Self-assembly and mineralization of peptide-amphiphile nanofibers. *Science 294*, 1684−1688.
(30) Shimizu, T.; Hato, M. (1993) Self-assembling properties of synthetic peptidic lipids. *Biochim. Biophys. Acta 1147*, 50−58.
(31) Hartgerink, J. D.; Beniash, E.; Stupp, S. I. (2002) Peptide-amphiphile nanofibers: a versatile scaffold for the preparation of self-assembling materials. *Proc. Natl. Acad. Sci. U.S.A. 99*, 5133−5138.
(32) Vernille, J. P.; Schneider, J. W. (2004) Sequence-specific oligonucleotide purification using peptide nucleic acid (PNA) amphiphiles in hydrophobic interaction chromatography. *Biotechnol. Prog.* in press.
(33) Yu, Y. C.; Tirrell, M.; Fields, G. B. (1998) Minimal lipidation stabilizes protein-like molecular architecture. *J. Am. Chem. Soc. 120*, 9979−9987.
(34) Chu-Kung, A. F.; Bozzelli, K. N.; Lockwood, N. A.; Haseman, J. R.; Mayo, K. H.; Tirrell, M. V. (2004) Promotion of peptide antimicrobial activity by fatty acid conjugation. *Bioconjugate Chem. 15*, 530−535.
(35) Ratilainen, T.; Holmen, A.; Tuite, E.; Haaima, G.; Christensen, L.; Nielsen, P. E.; Nordén, B. (1998) Hybridization of peptide nucleic acid. *Biochemistry 37*, 12331−12342.
(36) Ljungstrøm, T.; Knudsen, H.; Nielsen, P. E. (1999) Cellular uptake of adamantyl conjugated peptide nucleic acids. *Bioconjugate Chem. 10*, 955−972.
(37) Egholm, M.; Buchardt, O.; Nielsen, P. E.; Berg, R. H. (1992) Peptide nucleic acids (PNA). Oligonucleotide analogues with an achiral peptide backbone. *J. Am. Chem. Soc. 114*, 1895−1897.
(38) Chan, W. C.; White, P. D. (2000) *Fmoc Solid-Phase Peptide Synthesis*, Oxford University Press, New York.
(39) Nielsen, P. E., Egholm, M., Eds. (1999) *Peptide Nucleic Acids Protocols and Applications*, Horizon Scientific Press, Wymondham, U.K.
(40) Christensen, L.; Fitzpatrick, R.; Gildea, B.; Petersen, K. H.; Hansen, H. F.; Koch, T.; Egholm, M.; Buchardt, O.; Nielsen, P. E.; Coull, J. (1995) Solid-phase synthesis of peptide nucleic acids. *J. Pept. Sci. 1*, 185−183.
(41) Berndt, P.; Fields, G. B.; Tirrell, M. (1995) Synthetic lipidation of peptides and amino acids: monolayer structure and properties. *J. Am. Chem. Soc. 117*, 9515−9522.
(42) Egholm, M.; Casale, R. A. (2000) The chemistry of peptide nucleic acids. In *Solid-Phase Synthesis* (Kates, S. A., Albericio, F., Eds.) pp 549−578, Dekker, New York.
(43) Evans, D. F.; Wennerström, H. (1994) *The Colloidal Domain: Where Physics, Chemistry, Biology, and Technology Meet*, VCH Publishers, New York.
(44) Griffin, T. J.; Smith, L. M. (1998) An approach to predicting the stabilities of peptide nucleic acid:DNA duplexes. *Anal. Biochem. 260*, 56−63.
(45) Giesen, U.; Kleider, W.; Berding, C.; Geiger, A.; Ørum, H.; Nielsen, P. E. (1998) A formula for the thermal stability (T_m) prediction of PNA/DNA duplexes. *Nucleic Acids Res. 26*, 5004−5006.
(46) SantaLucia, J.; Allawi, H. T.; Seneviratne, P. A. (1996) Improved nearest-neighbor parameters for predicting DNA duplex stability. *Biochemistry 35*, 3555−3562.
(47) Anderson, C. F.; Record, M. T. (1983) *Structure and Dynamics* ed. (Clementi, E., Sarma, R, Eds.) pp 301−309, Adenine Press, New York.
(48) Bond, J. P.; Anderson, C. F.; Record, M. T. (1994) Conformational transitions of duplex and triplex nucleic acid helixes: thermodynamic analysis of effects of salt concentration on stability using preferential interaction coefficients. *Biophys. J. 67*, 825−836.
(49) Record, M. T.; Anderson, C. F.; Lohman, T. M. (1978) Thermodynamic analysis of ion effects on the binding and conformational equilibriums of proteins and nucleic acids: the roles of ion association or release, screening, and ion effects on water activity. *Q. Rev. Biophys. 11*, 103−178.
(50) Datta, B.; Armitage, B. A. (2001) Hybridization of PNA to structured DNA targets: quadruplex invasion and the overhang effect. *J. Am. Chem. Soc. 123*, 9612−9619.

BC049831A